nature nanotechnology

PROGRESS ARTICLE

PUBLISHED ONLINE: 5 AUGUST 2013 | DOI: 10.1038/NNANO.2013.144

# Low-frequency 1/*f* noise in graphene devices

Alexander A. Balandin

**Low-frequency noise with a spectral density that depends inversely on frequency has been observed in a wide variety of systems including current fluctuations in resistors, intensity fluctuations in music and signals in human cognition. In electronics, the phenomenon, which is known as 1/*f* noise, flicker noise or excess noise, hampers the operation of numerous devices and circuits, and can be a significant impediment to the development of practical applications from new materials. Graphene offers unique opportunities for studying 1/*f* noise because of its two-dimensional structure and widely tunable two-dimensional carrier concentration. The creation of practical graphene-based devices will also depend on our ability to understand and control the low-frequency noise in this material system. Here, the characteristic features of 1/*f* noise in graphene and few-layer graphene are reviewed, and the implications of such noise for the development of graphene-based electronics including high-frequency devices and sensors are examined.**

Low-frequency noise with the spectral density $S(f) \sim 1/f^{\gamma}$ (where $f$ is the frequency and $\gamma \approx 1$ is an experimental parameter) was discovered in vacuum tubes[1] and later observed in a diverse array of systems[2–5]. In electronics, this type of noise, which is commonly referred to as 1/*f* noise, flicker or excess noise, is usually found at $f < 100$ kHz. The corner frequency, $f_o$, where the 1/*f* noise level is equal to that of thermal or shot noise, ranges from a few Hz to tens of kHz and is often used as a figure of merit for the 1/*f* noise amplitude. The importance of 1/*f* noise in electronics has motivated numerous studies of its physical mechanisms and the development of a variety of methods for its reduction[6]. However, despite almost a century of research, 1/*f* noise remains a controversial phenomenon and numerous debates continue about its origin and mechanisms.

The common name for this intrinsic noise type does not imply the existence of a single physical mechanism that gives rise to all its manifestations[7]. It is now accepted that different fluctuation processes can be responsible for the 1/*f* noise in different materials and devices. For this reason, practical applications of a new material system usually require a thorough investigation of the specific features of the low-frequency noise in the material and the development of methods for its reduction. For example, the introduction of GaN/AlGaN wide-bandgap semiconductors into communication technologies relied on reducing the level of 1/*f* noise by about five orders of magnitude, which was achieved through several years of research and development[6,8].

Fluctuations in the electrical current, $I \propto qN\mu$, can be written as $\delta I \propto q(\delta N)\mu + qN(\delta\mu)$, where $q$ is the charge of an electron, $N$ is the number of charge carriers and $\mu$ is the mobility. Correspondingly, the mobility-fluctuation and carrier-number-fluctuation mechanisms of 1/*f* noise can be distinguished[7]. Box 1 provides a summary of the types of intrinsic noise and fundamentals of 1/*f* noise theory. It is generally accepted that in conventional semiconductor devices such as Si complementary metal–oxide–semiconductor (CMOS) field-effect transistors (FETs), 1/*f* noise is described well by the McWhorter model, which uses the carrier-number-fluctuation approach (see equation (1)). In metals, on the other hand, 1/*f* noise is usually attributed to fluctuations in mobility, which can arise from fluctuations in the scattering cross-section of scattering centres (equation (2)). There are materials and devices where contributions from both mechanisms are comparable or cross-correlated. The location of the noise sources — surface versus volume of the electrical conductor — has also been a subject of considerable debates[7,9–12].

Graphene is a unique material system in the context of 1/*f* noise owing to its two-dimensional (2D) nature, unusual linear energy dispersion for electrons and holes, zero-energy bandgap, specific scattering mechanisms and metallic-type conductance. On the one hand, it is an ultimate surface where conduction electrons are exposed to the traps, for example, charged impurities in a substrate or on its top surface, which can result in strong carrier-number fluctuations. On the other hand, graphene can be considered a zero-bandgap metal, where mobility fluctuations resulting from the charged scattering centres in the substrate or surface can also make a strong contribution to 1/*f* noise. The ability to change the thickness of few-layer graphene (FLG) conductors by one atomic layer at a time opens up opportunities for examining surface and volume contributions to 1/*f* noise directly.

## Importance of 1/*f* noise for graphene applications

In addition to the scientific significance of investigating 1/*f* noise in a 2D system, there are practical reasons why the 1/*f* noise characteristics of graphene are particularly important. They are related to graphene's physical properties and envisaged applications[13]. The most promising electronic applications of graphene are likely to be those that are not strongly hampered by the absence of the energy bandgap but rather rely on its exceptionally high electron mobility, thermal conductivity, saturation velocity and the possibility of tuning the carrier concentration, $n_C$, with the gate voltage over an exceptionally wide range. The applications that fall into this category are chemical and biological sensors, transparent electrodes, ultrafast transistors for communications, optoelectronic devices and interconnect wiring. Indeed, the exceptional sensitivity of graphene gas sensors has been demonstrated using the relative resistance of the graphene channels, $\Delta R/R$ (ref. 14). The sensitivity was attributed to the precise control of $n_C$ with the electrostatic gating and high $\mu$. The prospects of high-frequency graphene devices for communication, which rely on its high $\mu$ and saturation velocity, also look promising[15–17]. The symmetry of the electron band structure and wide variation of the carrier density were used to increase the functionality of amplifiers and phase detectors utilized in communications and signal processing[17]. For all mentioned applications, 1/*f* noise is a crucial performance metric.

Nano-Device Laboratory, Department of Electrical Engineering, Materials Science and Engineering Program, Bourns College of Engineering, University of California — Riverside, Riverside, California 92521, USA.
e-mail: balandin@ee.ucr.edu



© 2013 Macmillan Publishers Limited. All rights reserved

**Box 1 | Intrinsic noise types and fundamentals of 1/*f* noise.**

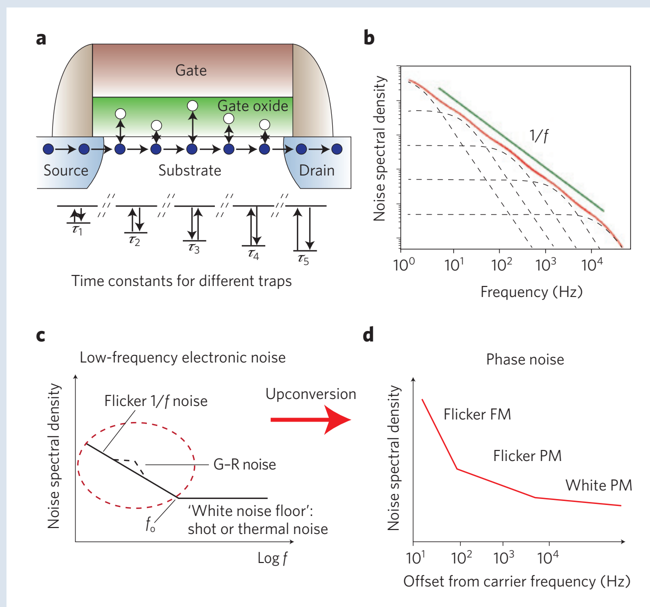


Various manifestations of electronic noise are commonly classified into four intrinsic types: (1) thermal or Johnson noise, (2) shot noise, (3) generation–recombination (G–R) noise and (4) flicker or 1/*f* noise[6]. The spectral density of thermal noise is given by Nyquist's formula $S_I(f) = 4k_BT/R$, where $k_B$ is Boltzmann's constant and $T$ is temperature. The spectral density of shot noise is given by Schottky's theorem $S_I(f) = 2q\langle I\rangle$, where $\langle I\rangle$ is the average value of the electrical current. Thermal and shot noise types have their origin in the random motion of charge carriers. Both types of noise are called white noise because their spectral density does not depend on $f$. Generation–recombination noise is observed at low $f$ and its spectral density is described by the Lorentzian: $S_I(f) = S_0/[1 + (2\pi f\tau)^2]$, where $S_0$ is the frequency independent portion of $S_I(f)$ observed at $f < (2\pi\tau)^{-1}$ and $\tau$ is the time constant associated with a specific trapping state (for example, ionized impurity). Unlike other types of intrinsic noise, 1/*f* noise can originate from different fluctuation processes either in $N$ or $\mu$, or from both.

The most common description of 1/*f* noise, dominated by fluctuations in $N$, stems from the observation that a superposition of individual G–R noise sources with the lifetime distributed on a logarithmically wide timescale, within the $\tau_1$ and $\tau_2$ limits, gives the 1/*f* spectrum in the intermediate range of frequencies $1/\tau_2 < \omega < 1/\tau_1$ (ref. 57). Here $\omega = 2\pi f$ is an angular frequency. Introducing a density distribution of lifetimes, $g(\tau_N)$, one can write the spectral density of the number fluctuations, $S_N$, in the form

$$S_N(\omega) = 4\overline{\delta N^2} \int_{\tau_1}^{\tau_2} g(\tau_N) \frac{\tau_N}{1 + (\omega\tau_N)^2} d\tau_N \qquad (1)$$

Integration of equation (1) for $g(\tau_N) = [\tau_N \ln(\tau_2/\tau_1)]^{-1}$ gives the 1/*f* spectrum inside the region determined by the limiting values of $\tau_N$. Further development of this idea in the context of semiconductors led to a model — commonly referred to as McWhorter's model[58] — that is used to describe 1/*f* noise in conventional FETs. Consider a typical Si CMOS device structure shown in **a**. Defects that act as the carrier traps are distributed inside a $SiO_2$ gate-oxide layer. Each defect is characterized by its own time constant $\tau_N$, which is determined by its distance from the channel, for example, $\tau = \tau_0 \exp(\lambda z)$, where $z$ is the distance of the trap from the channel, $\tau_0 \sim 10^{-10}$ s and $\lambda \sim 2 \times 10^8$ cm$^{-1}$ is the tunnelling parameter[58,59]. Carrier capture and emission back to the channel leads to current fluctuations $\delta I \propto q(\delta N)\mu$. The contribution of traps with different $\tau$ results in a set of G–R bulges represented by Lorentzian functions. The envelope of the closely positioned Lorentzians has the 1/*f*-type dependence over the relevant frequency range (**b**). If one type of traps dominates the fluctuation processes, for example, traps at the interface with the same time constant, the G–R bulge associated with this trapping state can appear superimposed on the 1/*f* spectrum (**c**). In the case of graphene, G–R noise was discussed in refs 23,60. The 1/*f* spectrum reaches the white noise floor at some $f_0$ (**c**). The oval shows a range where the noise is of 1/*f* type. Depending on a particular device or temperature, the white noise level is defined by either thermal or shot noise. Specifics of shot noise in graphene were reported in refs 61–65. An approach to re-cast the McWhorter model of 1/*f* noise specifically for graphene was reported in ref. 66. It was suggested that the observed noise in graphene correlates better with charge scattering primarily due to the long-range Coulomb scattering from charged impurities rather than short-range scattering from lattice defects[66].

The low-frequency 1/*f* noise caused by mobility fluctuations can appear as a result of the superposition of elementary events in which the scattering cross-section, $\sigma$, of the scattering centres fluctuates from $\sigma_1$ to $\sigma_2$. The cross-section can change owing to capture or release of the charge carriers. In the framework of the mobility-fluctuation model, the noise spectral density of the elemental fluctuation events contributing to 1/*f* noise in any material is given by[67–69]

$$\frac{S_I}{I^2} \propto \frac{N_t^\mu}{V} \frac{\tau\varsigma(1-\varsigma)}{1+(\omega\tau)^2} \Lambda^2 (\sigma_2 - \sigma_1)^2 \qquad (2)$$

where $N_t^\mu$ is the concentration of the scattering centres of a given type that contribute to the noise, $\Lambda$ is the mean free path of the charge carriers, $\zeta$ is the probability for a scattering centre to be in the state with $\sigma_1$. Integration of equation (2) results in the 1/*f* spectrum caused by the mobility fluctuations.

The absence of a single noise mechanism complicates an introduction of a meaningful figure of merit for 1/*f* noise. The most commonly used figure of merit — Hooge parameter, $\alpha_H$, — is based on his empirical formula[9]

$$S_R/R^2 = \alpha_H/Nf \qquad (3)$$

where $S_R \sim (\delta R)^2$ is the power spectral density of the fluctuations in the value of the resistance ($S_R/R^2 = S_I/I^2 = S_V/V^2$) and $V$ is the voltage. Equation (3) was introduced specifically for the mobility fluctuations but then extended to other 1/*f* noise mechanisms for the purpose of noise level comparison. The application of this figure of merit introduced for volume noise to a 2D system such as graphene presents conceptual difficulties.

Although 1/*f* noise dominates the spectrum only at low-frequency, it upconverts to high frequencies, because of unavoidable nonlinearities in the devices or systems (**d**). As a result, 1/*f* noise makes up the main contribution to the phase noise of communication systems and sensors (**d**; PM, phase modulation; FM, frequency modulation). Downscaling of any material system for use in nanometre-scale devices can further increase 1/*f* noise levels and complicate practical applications[50,70].



© 2013 Macmillan Publishers Limited. All rights reserved

The sensitivity of amplifiers and transducers used in sensors is ultimately defined by the low-frequency noise level[18,19]. The accuracy of a system limited by $1/f^{\gamma}$ noise cannot be improved by extending the measuring time, $t \propto 1/f$, if $\gamma \geq 1$. The energy, $E$, of a measured signal can be written as an integral of the square of its amplitude spectrum $E \propto (1/f^{\gamma})^2 df$ (ref. 18). It is seen from this integral that for $\gamma \geq 1$, the total accumulated energy of the flicker noise increases at least as fast as $t$. In contrast, when measuring white noise, for example, shot or thermal noise, the accuracy increases as $t^{1/2}$. The sensitivity and selectivity of many types of sensor, particularly those that rely on an electrical response, is limited by $1/f$ noise[18–20]. The same considerations apply to graphene sensors.

Although $1/f$ noise dominates the spectrum only at low frequencies, its level is important for communications applications at high frequencies, because $1/f$ noise is the main contributor to the phase noise of the oscillating systems (see Box 1). The phase noise of an oscillator, that is, spectral selectivity, determines a system's ability to separate adjacent signals. The upconversion of $1/f$ noise is a result of unavoidable nonlinearities in the electronic systems, which leads to $(1/f)^3$ phase noise contributions[19]. The level of $1/f$ noise is important for determining the competitiveness of graphene technology for cell phones, radars or other communication applications. These considerations explain the practical needs for a detailed investigation of $1/f$ noise in graphene devices.

## Characteristics of 1/*f* noise in graphene

The first reports of $1/f$ noise in graphene appeared in 2008[21,22]. They were quickly followed by a large number of studies of $1/f$ noise in graphene and FLG devices of different configurations and under various biasing conditions[23–38]. Despite major progress in the investigation of $1/f$ noise in graphene, many issues remain the subject of considerable debate. The latter is expected considering the time it took to gain understanding of $1/f$ noise in other, more conventional, materials[6]. Here we summarize the $1/f$ noise characteristics of graphene, which can be considered commonly accepted or reproducibly measured in different laboratories.

Published reports agree that the low-frequency noise in graphene is scale-invariant and reveals a $1/f$ spectral dependence with $f_o$ in the range ~1 to 100 kHz, which is similar to metals and semiconductors[21–36]. Figure 1a–f shows typical $1/f$ noise characteristics of graphene devices. In a few instances generation–recombination-type bulges were observed in the low-frequency noise spectrum[23]. They were attributed to defects on the edges of graphene channels, with some characteristic time constants, which dominated the fluctuations. The noise spectral density $S_I$ is proportional to $I^2$ in graphene and implies that the electrical current $I$ does not drive the fluctuations, but merely makes the fluctuations in the sample visible if Ohm's law is used[7]. Measurements of $1/f$ noise in graphene devices with large variations of the channel area, $W \times L$ (where $W$ is the width and $L$ is the length), from ~1 to 80 μm², confirmed that $1/f$ noise mostly originates from graphene itself and is not dominated by contributions from the metal contacts[36].

Together with the normalized noise spectral density, $S_I/I^2$, the noise amplitude, $A = (1/N)\Sigma_{m=1}^{N} f_m S_{Im}/I_m^2$, can be used to characterize $1/f$ noise levels (here $S_{Im}$ and $I_m$ are the noise spectral density and drain–source current measured at $m$ different frequencies $f_m$). This definition helps to reduce measurement error at specific frequencies[21,22]. The measurements of $1/f$ noise in graphene revealed that its amplitude is relatively low[21–32]. This may seem surprising considering that graphene has the thickness of just one atomic layer and carriers in graphene are ultimately exposed to disorder and traps in the gate oxide or on its surface. Different groups reported consistent values of $S_I/I^2$ in the range $10^{-9}$ to $10^{-7}$ Hz$^{-1}$ at $f = 10$ Hz or $A \sim 10^{-9}$ to $10^{-7}$ for micrometre-scale channels[21–32]. The noise normalized to the channel area $(S_I/I^2)(W \times L)$ is ~$10^{-8}$ to $10^{-7}$ μm² Hz$^{-1}$ for micrometre-scale graphene devices.

Most reports are in agreement that $1/f$ noise in graphene reveals an unusual gate-bias dependence[28,30,32,36–38]. Close to the Dirac point, the noise amplitude follows a V-shape dependence attaining its minimum at the Dirac point where the resistance is at its maximum (Fig. 1c). This dependence was reported independently by several groups using graphene devices, which varied in their design and the way they were fabricated. In some devices, V-shape dependence became M-shape over the extended bias range[28,36–38]. There are several proposed explanations of V- and M-shape gate-bias dependence[28,30,32,37]. In ref. 28, the authors attributed M-shape dependence of the noise amplitude to the spatial charge inhomogeneity related to the presence of the electron and hole puddles in graphene. Another explanation originated from the observation that M-type behaviour before annealing transformed to V-type after annealing, irrespective of the changes in $\mu$ of the graphene samples[37]. The transformation was attributed to the interplay between the long- and short-range scattering mechanisms. Water contamination of the graphene surface was found to significantly enhance the noise magnitude and change the type of noise behaviour. Removal of water by annealing resulted in the suppression of the long-range scattering[37].

The unusual gate dependence of the noise amplitude in graphene observed in many experiments supports the conclusion that $1/f$ noise in graphene devices does not follow the McWhorter model conventionally used for Si CMOS devices and other metal–oxide–semiconductor field-effect transistors (MOSFETs). The McWhorter model predicts that $S_I/I^2$ decreases in the inversion regime as $\sim(1/n_C)^2$ (refs 36,39–40). Any deviation from this behaviour is interpreted as the influence of the contacts, inhomogeneous trap distribution in energy or space, or contributions of the mobility fluctuations to the noise[39,40]. Figure 1e shows the McWhorter model predictions for the normalized noise amplitudes calculated for different trap concentrations. The regions between lines 1 and 2 and between lines 2 and 3 correspond to the typical noise levels in regular Si n-channel MOSFETs and in Si MOSFETs with high-κ dielectric, respectively[36]. The shaded region represents the results for the noise spectral density measured in graphene FETs. With a large $n_C$, noise in graphene is higher than in typical Si MOSFETs, whereas a small $n_C$ yields a noise level in graphene FETs that is lower than in Si MOSFETs. Despite the immature state of graphene technology, the noise level in graphene FETs are comparable to that in Si MOSFETs.

A recent study explained the observed carrier-density-dependence of $1/f$ noise in graphene within the mobility-fluctuation approach (using an expression originating from equation (2)) and taking into account the gate-bias dependence of the electron mean free path, $\Lambda$, and the scattering cross sections $\sigma_1$ and $\sigma_2$ of the long-range and short-range scattering centres[41]. An independent investigation of $1/f$ noise in a wide selection of graphene devices ($\mu$ in the range 400 to 20,000 cm² V$^{-1}$ s$^{-1}$) concluded that in most of the devices examined the dominant contribution to $1/f$ noise was from the mobility fluctuations arising from the fluctuations in the scattering cross-section $\sigma$ (ref. 38). The authors termed this noise mechanism 'configuration noise' with the noise density proportional to $\Lambda^2\sigma^2$ (ref. 38). This model is similar to the one reported in ref. 41 and is consistent with equation (2). One should note that the carrier-number and mobility-fluctuation mechanisms can be closely related because the fluctuations in $\sigma$ of the scattering centres can be due to the capture or emission of electrons, which also changes $N$.

The $1/f$ noise dependence on the number of atomic planes, $n_a$, in FLG devices can shed light on the physical mechanism of $1/f$ noise. It is also important for practical applications. Increasing $n_a$ reduces $\mu$ and complicates gating. The benefits of a larger $n_a$ in FLG include larger currents and a weaker influence of traps inside the gate dielectrics on the electron transport inside an FLG channel. It was reported that the noise in bilayer graphene (BLG) channels is lower than in single-layer graphene (SLG; ref. 21). The authors suggested that $1/f$ noise reduction in BLG is associated with its band structure



© 2013 Macmillan Publishers Limited. All rights reserved

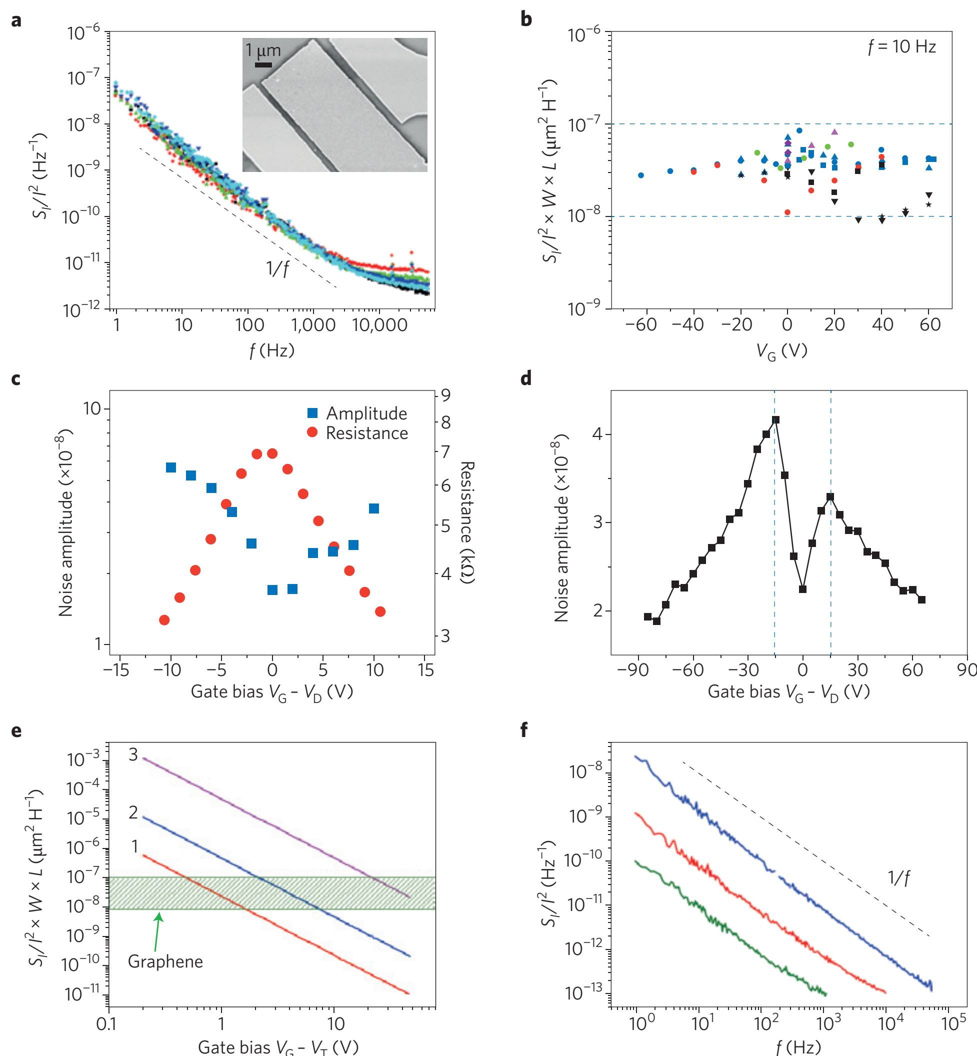


**Figure 1 | Noise characteristics of graphene devices. a**, $S_I/I^2$ of a top-gated graphene device as a function of $f$ for a range of gate biases $V_G$ = 0–40 V. The source–drain voltage is $V_{DS}$ = 50 mV. The inset shows a scanning electron microscopy image of the top-gated graphene FET. TLG, trilayer graphene. **b**, $S_I/I^2$ in different graphene devices normalized by the graphene channel area $W \times L$ as a function of $V_G$. The data points in blue (circles, triangles and rectangles) are for three SLG devices whereas the rest of the data points are for BLG devices. **c**, Graph showing noise amplitude and channel resistance as a function of the gate bias. The data shows the V-type noise behaviour consistent with many independent reports. $V_D$, Dirac voltage. **d**, Experimental M-shape dependence of 1/$f$ noise spectral density on the gate bias reported in several studies. The vertical lines indicate the carrier concentration $n_C$ ~$10^{12}$ cm$^{-2}$. **e**, $S_I/I^2$ multiplied by the graphene channel area as a function of the gate bias. $V_T$, threshold voltage. The lines are calculated from the McWhorter model for three different gate-oxide trap concentrations: (1) $N_T = 5 \times 10^{16}$ (cm$^3$ eV)$^{-1}$, (2) $N_T = 10^{18}$ (cm$^3$ eV)$^{-1}$ and (3) $N_T = 10^{20}$ (cm$^3$ eV)$^{-1}$. The dashed region represents the experimental noise level for graphene transistors. The frequency of the analysis is $f$ = 10 Hz. The data indicates that 1/$f$ noise in graphene does not follow a $(1/n_C)^2$ dependence characteristic for conventional FETs. **f**, $S_I/I^2$ as a function of $f$ in FLG shown for three devices with distinctly different thicknesses defined by the number of atomic planes $n$ = 1 (blue), $n \approx 7$ (red) and $n \approx 12$ (green). Figure reproduced with permission from: **a**, ref. 24, © 2009 AIP; **b**,**e**, ref. 36, © 2010 IOP; **c**, ref. 49, © 2013 AIP; **d**, ref. 51, © 2010 ACS; **f**, ref. 44, © 2013 AIP.

that varies with the charge distribution between the two atomic planes resulting in screening of the potential fluctuations owing to the external impurity charges[21]. It was later confirmed that the 1/$f$ noise level continues to decrease with increasing thickness of FLG conductors. Figure 1f shows the experimentally determined trend for noise reduction with increasing $n_a$, that is, the channel thickness $H = n_a \times h$, where $h$ = 0.35 nm is the thickness of SLG.

The noise from the volume of a sample originated from independent fluctuators scaled inversely proportional to the sample volume. Therefore, for the constant area film, noise is inversely proportional to its thickness $H$ as $S_I/I^2 \propto 1/H$. Such dependence observed experimentally can be interpreted as an indication of a volume–noise mechanism[9,42]. If noise originates from the surface, varying the thickness of the film serves only to change the fraction of $I$ passing through the surface layer. Then the 1/$f$ noise would depend on the thickness according to $S_I/I^2 \propto (1/H)^2$ (refs 12,43). Previous attempts to test directly whether 1/$f$ noise is dominated by contributions coming from the sample surface or its volume have not led to conclusive answers because of the inability to fabricate continuous metal or semiconductor films with a uniform thickness below ~8 nm (ref. 12). Unlike the thickness of metal or semiconductor films, the thickness of FLG can be continuously and uniformly varied all the way down to a single atomic layer — the actual surface. It was recently found that 1/$f$ noise in FLG becomes dominated by the volume noise when the thickness exceeds $n_a$ ~7 (~2.5 nm; ref. 44). The 1/$f$ noise is the surface phenomenon below this thickness. At the high-bias regime, the surface contributions are pronounced even for larger $H$ (ref. 44).



© 2013 Macmillan Publishers Limited. All rights reserved

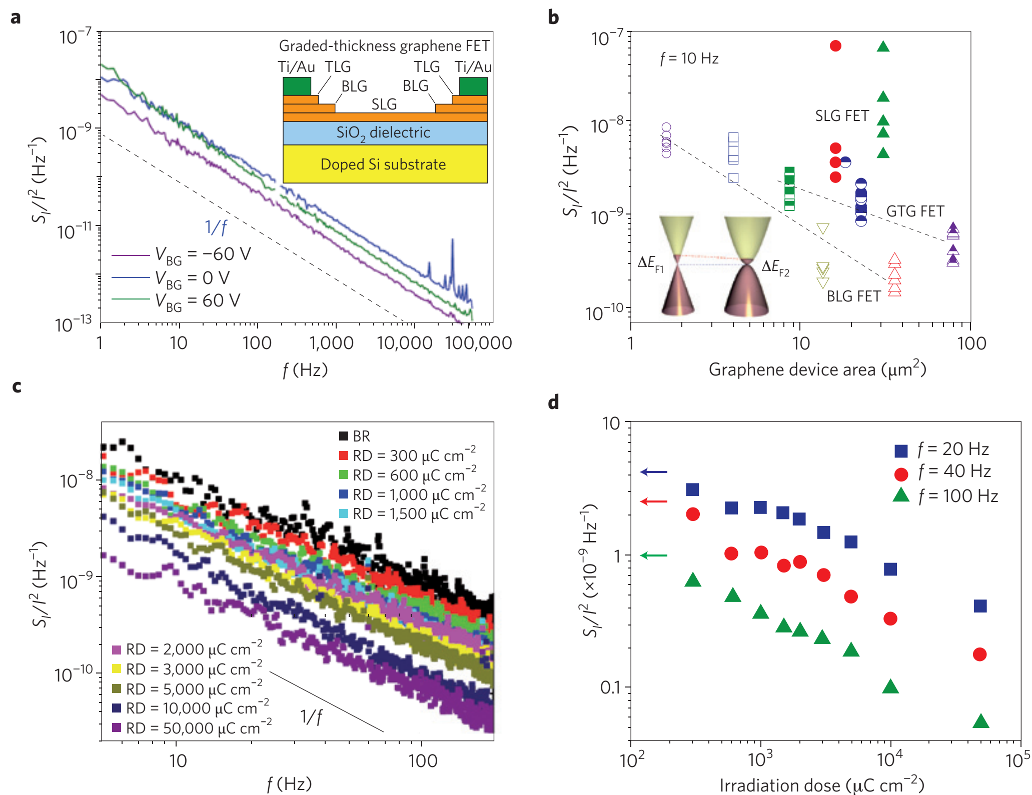


**Figure 2 | Noise reduction in graphene devices. a**, $S_I/I^2$ in a typical back-gated graphene device. The inset illustrates the design of the graded-thickness graphene (GTG) FET with the channel thickness gradually changing from graphene to FLG near the metal contacts. **b**, $S_I/I^2$ of GTG FETs, and the reference SLG and BLG FETs as a function of the graphene channel area. The filled symbols represent SLG, the open symbols BLG and the half-filled symbols GTG FETs. For each device the data are shown at several biasing points within the $|V_G–V_D| \leq 30$ V range from the Dirac point. The dashed lines are guides to the eye. Note that GTG FETs have a comparably reduced noise level to that observed in BLG FETs, and reveal an electron mobility that is almost as high as in graphene FETs. The inset shows the band structures of SLG with the linear dispersion, and BLG with the parabolic dispersion in the vicinity of the charge neutrality point. $\Delta E_{F1}$ and $\Delta E_{F2}$ are shifts in the Fermi energy positions due to electron transfer between the metal contact and graphene for SLG and BLG, respectively. **c**, $S_I/I^2$ as a function of *f* for a graphene device after each irradiation step. The source–drain bias was varied from 10 to 30 mV. The data before irradiation is marked as BR. Note that 1/*f* noise decreases monotonically with increasing irradiation dose indicated as RD. $V_{BG}$, back-gate voltage. **d**, $S_I/I^2$ as a function of the irradiation dose at zero gate bias. The arrows indicate the level of 1/*f* noise before irradiation. Figure reproduced with permission from: **a**,**b**, ref. 47, © 2012 AIP; **c**,**d**, ref. 49, © 2013 AIP.

## Noise reduction in graphene devices

The noise amplitudes of ~$10^{-9}$ to $10^{-7}$ reported for micrometre-sized graphene channels are relatively low. A comparison with carbon nanotubes shows that graphene devices have lower resistance and about three orders of magnitude smaller noise amplitude[45]. Environmental exposure and ageing increased the level of 1/*f* noise[36]. Deposition of the top-dielectric in the top-gate of graphene FETs results in mobility degradation but does not substantially increase the noise level[24]. This suggests that the use of the high-quality cap layers on top of graphene channels may prevent an increase of 1/*f* noise when exposed to environmental factors, such as water vapour or organic contaminations. Practical applications of graphene, particularly in low-power devices with nanometre-scale channels, will require further reduction in the 1/*f* noise level. It is generally true that as the technology matures, the level of 1/*f* noise decreases[6]. A smaller density of structural defects and higher material quality usually results in smaller noise spectral density. Special processing steps or device designs can lead to a substantial reduction in the noise level. For example, it was shown that GaN/AlGaN heterostructure field-effect transistors (HFETs) where the high current density is achieved by increasing Al content in the barrier layer — so-called piezo-doping — reveal a lower 1/*f* noise level than in GaN/AlGaN HFETs with conventional channel doping[46]. Several possible methods of 1/*f* noise reduction in graphene FETs have also been reported.

In one approach, the device channel was implemented with FLG where the thickness varied from SLG in the middle to BLG or FLG at the source and drain contacts (Fig. 2a,b). It was found that such graded-thickness graphene (GTG) devices have $\mu$ comparable to the reference SLG devices while producing lower noise levels[47]. The electron density of states (DOS) in SLG in the vicinity of its Dirac point is low owing to the Dirac-cone linear dispersion. Even a small amount of the charge transfer from or to the metal can strongly affect the Fermi energy, $E_F$, of graphene. The values of $\Delta E_F = -0.23$ eV and $\Delta E_F = 0.25$ eV were reported for Ti and Au contacts to graphene, respectively[48]. The quadratic energy dispersion in BLG or FLG results in DOS that is different from that in graphene. The same amount of charge transfer determined by the work function difference will lead to the smaller Fermi level shifts in BLG and FLG than in SLG owing to the larger DOS in BLG and FLG (see inset to Fig. 2a). The potential barrier fluctuations will be smaller at the metal/BLG or metal/FLG interface than in the metal/SLG interface, resulting in a lower noise level[47].

Another approach is related to the electron irradiation treatment of graphene channels[49]. It was recently reported that 1/*f* noise in graphene reveals an interesting characteristic — it reduces after irradiation (Fig. 2c,d). It was experimentally observed that bombardment of graphene devices with low-energy 20-keV electrons, which induce defects but do not eject carbon atoms, can reduce $S_I/I^2$ by an order of magnitude at a radiation dose of $10^4$ μC cm$^{-2}$ (ref. 49). It was indicated



© 2013 Macmillan Publishers Limited. All rights reserved

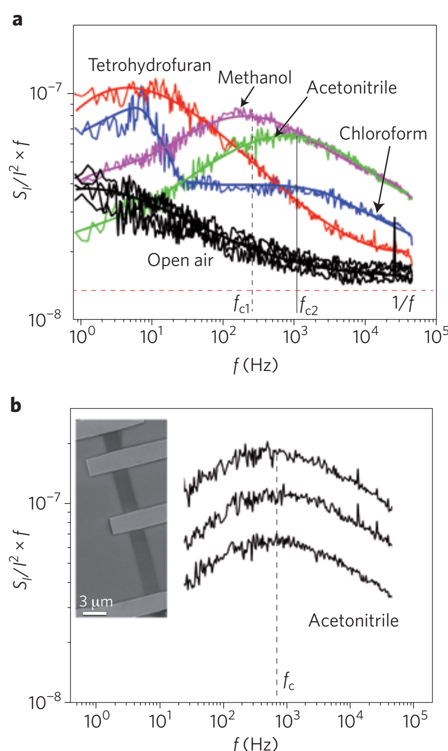


**Figure 3 | Low-frequency noise as a sensing signal. a**, $S_I/I^2$ multiplied by $f$ versus $f$ for the device in open air and under the influence of different vapours. Different vapours induce noise with different characteristic frequencies, $f_c$, and are shown explicitly for two different gases. The solid lines show the polynomial fitting of the experimental data. **b**, $S_I/I^2$ multiplied by $f$ versus $f$ for three different graphene devices exposed to acetonitrile vapour. Note the excellent reproducibility of the noise response of the graphene devices showing the same $f_c$ for all three devices. The inset shows a scanning electron microscopy image of the label-free graphene sensor. Figure reproduced with permission from ref. 56, © 2012 ACS.

that noise reduction in graphene under irradiation can be more readily interpreted within the mobility-fluctuation model. The electron-beam irradiation, while strongly reducing $\mu$ and, correspondingly, $\Lambda$, may not produce a major change in the number of scattering centres $N_t^\mu$ contributing to $1/f$ noise. This reduction in $\Lambda$ leads to an overall decrease of the $1/f$ noise level (equation (2)). In graphene, $\mu$ is limited by the long-range Coulomb scattering from charged defects even at room temperature, in contrast to semiconductors or metals, where $\mu$ at room temperature is typically limited by phonons, even if the defect concentration is high. The latter can explain why the effect produced by electron irradiation on $1/f$ noise in graphene differs from that in conventional materials. The noise reduction comes at the expense of mobility degradation. However, this trade-off is feasible as $\mu$ after irradiation still remains sufficiently high for practical applications.

## Challenges and opportunities

The field of $1/f$ noise in graphene is still far from being mature. It experienced a surge in the number of experimental reports and various models proposed for explanations of particular aspects of $1/f$ noise in graphene. The challenges that have to be addressed to facilitate the development of graphene technology are the following. First, there is a need to develop a comprehensive theory, which would explain the unusual gate-bias dependence of $1/f$ noise in graphene. The developed theoretical models could then be incorporated in computer-aided design tools used for optimizing graphene device structure. Second, the influence of metal contacts, surface contamination or analyte molecules attached to graphene channels on the low-frequency noise characteristics have to be closely examined. Considering that the electronic applications and fabrication of sensor arrays require nanometre-scale devices the third important challenge would be to understand what happens to $1/f$ noise when the graphene channels' length and width are on the nanometre-length scale. It was established for conventional Si CMOS technology that the average $1/f$ noise level exhibits a much stronger than linear increase on reducing the device size[50]. The initial report of $1/f$ noise in graphene nanoribbons[51,52] found increased $A \sim 10^{-6}$ to $10^{-5}$, for ribbons with widths of ~40–70 nm (ref. 51). It was also suggested that the fluctuations in conductance are correlated with the electron DOS revealing peaks in the noise spectral density with the positions matching the electron sub-band energies[51,52]. In the devices where the width of graphene channels scales down to just a few nanometres one may need to consider the electron hopping transport regime and corresponding implications for $1/f$ noise. It is known that the level of $1/f$ noise in the 'hopping' conductors increases with decreasing temperature[53,54], which is opposite to what is normally observed in regular conductors. Finally, variability effects in graphene, originating from environmental disturbance, and material and process variations[55] have to be studied systematically and separated from the fundamental noise characteristics.

Although detrimental in many of its manifestations, low-frequency noise presents opportunities for materials characterization and can serve positive functions when used cleverly. Low-frequency noise spectroscopy can provide information about the trap levels and charge-carrier dynamics. It can also be used to detect degradation in interconnects. The low-frequency noise in graphene is no exception (Fig. 3). It was reported that the use of the $S_I/I^2$ fluctuation signal together with the resistance change $\Delta R/R$ in graphene sensors allows the selective detection of gas molecules without prior functionalization of their surfaces[56]. The same approach can be extended to label-free graphene biosensors. It is reasonable to expect more of such device concepts where the excellent electronic properties of graphene are complemented by its unusual noise characteristics. In terms of fundamental science, graphene–FLG constitutes a unique material system, which allows the evolution of $1/f$ noise to be investigated as the dimensionality changes from bulk to a 2D surface[44]. The implications of this investigation can go beyond graphene-related materials. Addressing these challenges and opportunities will allow graphene's potential to be fully exploited for ultrasensitive and selective sensors, and high-speed communication applications.

Received 13 January 2013; accepted 8 June 2013; published online 5 August 2013

## References

1. Johnson, J. B. The Schottky effect in low frequency circuits. *Phys. Rev.* **26,** 71–85 (1925).
2. Flinn, I. Extent of the 1/*f* noise spectrum. *Nature* **219,** 1356–1357 (1968).
3. Voss, R. F. & Clarke, J. 1/*f* noise in music and speech. *Nature* **258,** 317–318 (1975).
4. Gilden, D. L., Thornton, T. & Mallon, M. W. 1/*f* noise in human cognition. *Science* **267,** 1837–1839 (1995).
5. Schoelkopf, R. J., Wahlgren, P., Kozhevnikov, A. A., Delsing, P. & Prober, D. E. The radio-frequency single-electron transistor: A fast and ultrasensitive electrometer. *Science* **280,** 1238–1242 (1998).
6. Balandin, A. A. *Noise and Fluctuations Control in Electronic Devices* (American Scientific, 2002).
7. Dutta, P. & Horn, P. M. Low-frequency fluctuations in solids: 1/*f* noise. *Rev. Mod. Phys.* **53,** 497–516 (1981).
8. Balandin, A. *et al.* Low flicker-noise GaN/AlGaN heterostructure field-effect transistors for microwave communications. *IEEE Trans. Microwave Theory Tech.* **47,** 1413–1417 (1999).
9. Hooge, F. N. 1/*f* noise is no surface effect. *Phys. Lett. A* **29,** 139–140 (1969).
10. Mircea, A., Roussel, A. & Mitonneau, A. 1/*f* noise: Still a surface effect. *Phys. Lett. A* **41,** 345–346 (1972).



© 2013 Macmillan Publishers Limited. All rights reserved

11. Fleetwood, G. M., Masden, J. T. & Giordano, N. 1/*f* noise in platinum films and ultrathin platinum wires: Evidence for a common bulk origin. *Phys. Rev. Lett.* **50,** 450–453 (1983).
12. Zimmerman, D. M., Scofield, J. H., Mantese, J. V. & Webb, W. W. Volume versus surface origin of 1/*f* noise in metals. *Phys. Rev. B* **34,** 773–777 (1986).
13. Geim, A. K. & Novoselov, K. S. The rise of graphene. *Nature Mater.* **6,** 183–191 (2007).
14. Schedin, F. *et al.* Detection of individual gas molecules adsorbed on graphene. *Nature Mater.* **16,** 652–655 (2007).
15. Schwierz, F. Graphene transistors. *Nature Nanotech.* **5,** 487–496 (2010).
16. Meric, I. *et al.* Channel length scaling in graphene field-effect transistors studied with pulsed current–voltage measurements. *Nano Lett.* **11,** 1093–1097 (2011).
17. Yang, X., Liu, G., Rostami, M., Balandin, A. A. & Mohanram, K. Graphene ambipolar multiplier phase detector. *IEEE Electron. Dev. Lett.* **32,** 1328–1330 (2011).
18. Pettai, R. *Noise in Receiving Systems* (Wiley, 1984).
19. Motchenbacher, C. D. & Fitchen, F. C. *Low-Noise Electronic Design* (Wiley, 1973).
20. Potyrailo, R. A., Surman, C., Nagraj, N. & Burns, A. Materials and transducers toward selective wireless gas sensing. *Chem. Rev.* **111,** 7315–7354 (2011).
21. Lin, Y. M. & Avouris, P. Strong suppression of electrical noise in bilayer graphene nanodevices. *Nano Lett.* **8,** 2119–2125 (2008).
22. Chen, Z., Lin, Y. M., Rooks, M. J. & Avouris, P. Graphene nano-ribbon electronics. *Physica E* **40,** 228–232 (2007).
23. Shao, Q. *et al.* Flicker noise in bilayer graphene transistors. *IEEE Electron. Dev. Lett.* **30,** 288–290 (2009).
24. Liu, G. *et al.* Low-frequency electronic noise in the double-gate single-layer graphene transistors. *Appl. Phys. Lett.* **95,** 033103 (2009).
25. Pal, A. N. & Ghosh, A. Resistance noise in electrically biased bilayer graphene. *Phys. Rev. Lett.* **102,** 126805 (2009).
26. Pal, A. N. & Ghosh, A. Ultralow noise field-effect transistor from multilayer graphene. *Appl. Phys. Lett.* **95,** 082105 (2009).
27. Imam, S. A., Sabri, S. & Szkopek, T. Low-frequency noise and hysteresis in graphene field-effect transistors on oxide. *Micro Nano Lett.* **5,** 37–41 (2010).
28. Xu, G. *et al.* Effect of spatial charge inhomogeneity on 1/*f* noise behavior in graphene. *Nano Lett.* **10,** 3312–3317 (2010).
29. Cheng, Z., Li, Q., Li, Z., Zhou, Q. & Fang, Y. Suspended graphene sensors with improved signal and reduced noise. *Nano Lett.* **10,** 1864–1868 (2010).
30. Heller, I. *et al.* Charge noise in graphene transistors. *Nano Lett.* **10,** 1563–1567 (2010).
31. Rumyantsev, S. L., Liu, G., Shur, M. & Balandin, A. A. Observation of the memory steps in graphene at elevated temperatures. *Appl. Phys. Lett.* **98,** 222107 (2011).
32. Zhang, Y., Mendez, E. E. & Du, X. Mobility-dependent low-frequency noise in graphene field-effect transistors. *ACS Nano* **5,** 8124–8130 (2011).
33. Lee, S. K. *et al.* Correlation of low frequency noise characteristics with the interfacial charge exchange reaction at graphene devices. *Carbon* **50,** 4046–4051 (2012).
34. Robinson, J. T., Perkins, F. K., Snow, E. S., Wei, Z. & Sheehan, P. E. Reduced graphene oxide molecular sensors. *Nano Lett.* **8,** 3137–3140 (2008).
35. Grandchamp, B. *et al.* Characterization and modeling of graphene transistor low-frequency noise. *IEEE Trans. Electron. Dev.* **59,** 516–519 (2012).
36. Rumyantsev, S., Liu, G., Stillman, W., Shur, M. & Balandin, A. A. Electrical and noise characteristics of graphene field-effect transistors: ambient effects, noise sources and physical mechanisms. *J. Phys. Condensed Matter* **22,** 395302 (2010).
37. Kaverzin, A. A., Mayorov, A. S., Shytov, A. & Horsell, D. W. Impurities as a source of 1/*f* noise in graphene. *Phys. Rev. B* **85,** 075435 (2012).
38. Pal, A. N. *et al.* Microscopic mechanism of 1/*f* noise in graphene: Role of energy band dispersion. *ACS Nano* **5,** 2075–2081 (2011).
39. Celik-Butler, Z. & Hsiang, T. Y. Spectral dependence of noise on gate bias in n-MOSFETS. *Solid-State Electron.* **30,** 419–423 (1987).
40. Dmitriev, A. P., Borovitskaya, E., Levinshtein, M. E., Rumyantsev, S. L. & Shur, M. S. Low frequency noise in degenerate semiconductors. *J. Appl. Phys.* **90,** 301–305 (2001).
41. Rumyantsev, S. *et al.* Low-frequency noise in graphene field-effect transistors. *Proc. 21st Int. Conf. Noise and Fluctuations* (ICNF 2011) 234–237 (IEEE, 2011).
42. Hooge, F. N. 1/*f* noise. *Physica* **83,** 14–23 (1976).
43. Celasco, M. *et al.* Comment on 1/*f* noise and its temperature dependence in silver and copper. *Phys. Rev. B* **19,** 1304–1306 (1979).
44. Liu, G., Rumyantsev, S., Shur, M. S. & Balandin, A. A. Origin of 1/*f* noise in graphene multilayers: Surface vs. volume. *Appl. Phys. Lett.* **102,** 093111 (2013).
45. Liu, G., Stillman, W., Rumyantsev, S., Shur, M. & Balandin, A. A. Low-frequency electronic noise in graphene transistors: comparison with carbon nanotubes. *Int. J. High Speed Electronic Syst.* **20,** 161–170 (2011).
46. Balandin, A. *et al.* Effect of channel doping on the low-frequency noise in GaN/AlGaN heterostructure field-effect transistors. *Appl. Phys. Lett.* **75,** 2064–2066 (1999).
47. Liu, G., Rumyantsev, S., Shur, M. & Balandin, A. A. Graphene thickness-graded transistors with reduced electronic noise. *Appl. Phys. Lett.* **100,** 033103 (2012).
48. Lee, E. J., Balasubramanian, K., Weitz, R. T., Burghard, M. & Kern, K. Contact and edge effects in graphene devices. *Nature Nanotech.* **3,** 486–490 (2008).
49. Hossain, Md. Z., Roumiantsev, S. L., Shur, M. & Balandin, A. A. Reduction of 1/*f* noise in graphene after electron-beam irradiation. *Appl. Phys. Lett.* **102,** 153512 (2013).
50. Simoen, E. & Claeys, C. On flicker noise in submicron silicon MOSFETs. *Solid-State Electron.* **43,** 865–882 (1999).
51. Xu, G. *et al.* Enhanced conductance fluctuation by quantum confinement effect in graphene nanoribbons. *Nano Lett.* **10,** 4590–4594 (2010).
52. Xu, G. *et al.* Low-noise submicron channel graphene nanoribbons. *Appl. Phys. Lett.* **97,** 073107 (2010).
53. Kozub, V. I. Low-frequency noise due to site energy fluctuations in hopping conductivity. *Solid-State Commun.* **97,** 843–846 (1996).
54. Shklovskii, B. I. 1/*f* noise in variable range hopping conduction. *Phys. Rev. B* **67,** 045201 (2003).
55. Xu, G., Zhang, Y., Duan, X., Balandin, A. A. & Wang, K. L. Variability effects in graphene: challenges and opportunities for device engineering and applications. *Proc. IEEE* **99,** 1–19 (2013).
56. Rumyantsev, S., Liu, G., Shur, M. S., Potyrailo, R. A. & Balandin, A. A. Selective gas sensing with a single pristine graphene transistor. *Nano Lett.* **12,** 2294–2298 (2012).
57. Bernamont, J. *Fluctuations de potential aux bornes dun conducteur metallique de faible volume parcouru par un courant. Ann. Phys. Leipzig* **7,** 71 (1937).
58. McWhorter, A. L. & Kingston, R. H. *Semiconductor Surface Physics* (Univ. of Pennsylvania Press, 1957).
59. Surya, C. & Hsiang, T. Y. Theory and experiment on the 1/*fγ* noise in p-channel metal-oxide-semiconductor field-effect transistors at low drain bias. *Phys. Rev. B* **33,** 4898–4905 (1986).
60. Vasko, F. T. & Mitin, V. V. Generation and recombination processes via acoustic phonons in disordered graphene. *Phys. Rev. B* **84,** 155445 (2011).
61. DiCarlo, L., Williams, J. R., Zhang, Y., McClure, D. T. & Marcus, C. M. Shot noise in graphene. *Phys. Rev. Lett.* **100,** 156801 (2008).
62. Danneau, R. *et al.* Shot noise measurements in graphene. *Solid-State Commun.* **149,** 1050–1055 (2009).
63. Danneau, R. *et al.* Shot noise suppression and hopping conduction in graphene nanoribbons. *Phys. Rev. B* **82,** 16105 (2010).
64. Tworzydło, J., Trauzettel, B., Titov, M., Rycerz, A. & Beenakker, C. W. Sub-Poissonian shot noise in graphene. *Phys. Rev. Lett.* **96,** 246802 (2006).
65. Golub, A. & Horovitz, B. Shot noise in graphene with long-range Coulomb interaction and local Fermi distribution. *Phys. Rev. B* **81,** 245424 (2010).
66. Sun, N. *et al.* Electrical noise and transport properties of graphene. *J. Low Temp. Phys.* 1–10 (2013).
67. Galperin, Yu. M., Karpov, V. G. & Kozub, V. I. Low-frequency noise in disordered systems in a wide temperature range. *Sov. Phys. JETP* **68,** 648–653 (1989).
68. Galperin, Yu. M., Gurevich, V. L. & Kozub, V. I. Disorder-induced low-frequency noise in small systems: Point and tunnel contacts in the normal and superconducting state. *Europhys. Lett.* **10,** 753–758 (1989).
69. Dmitriev, A. P., Levinshtein, M. E. & Rumyantsev, S. L. On the Hooge relation in semiconductors and metals. *J. Appl. Phys.* **106,** 024514 (2009).
70. Mihaila, M. N. in *Noise and Fluctuations Control Electronic Devices* (ed. Balandin, A. A.) 367–385 (American Scientific, 2002).

## Acknowledgements

This work was supported, in part, by the Semiconductor Research Corporation (SRC) and Defence Advanced Research Project Agency (DARPA) through FCRP Center for Function Accelerated nanoMaterial Engineering (FAME), and by the National Science Foundation (NSF) projects CCF-1217382, EECS-1124733 and EECS-1102074. The author is indebted to S. Rumyantsev (RPI and Ioffe Institute) for critical reading of the manuscript and providing valuable suggestions. He also acknowledges insightful discussions on 1/*f* noise in graphene with M. Shur (RPI).

## Additional information

Reprints and permissions information is available online at www.nature.com/reprints. Correspondence should be addressed to A.A.B.

## Competing financial interests

The authors declare no competing financial interests.



© 2013 Macmillan Publishers Limited. All rights reserved